



Review

The Opportunities of Cellulose for Triboelectric Nanogenerators: A Critical Review

Renyun Zhang

Department of Engineering, Mathematics and Science Education, Mid Sweden University, Holmgatan 10, 85170 Sundsvall, Sweden; renyun.zhang@miun.se

Abstract: Engineering polymers stand out as the predominant dielectric materials in triboelectric nanogenerators (TENGs), primarily owing to their robust triboelectric effect and widespread availability. However, growing environmental concerns surrounding these polymers have prompted a notable shift towards exploring alternative eco-friendly materials, with cellulose materials emerging as compelling contenders over the past few years. Cellulose, derived from various sources and presented in diverse forms and structures, has found utility as triboelectric materials. In contrast to many engineering polymers known for their chemical stability, cellulose materials exhibit heightened chemical activities. This characteristic provides a unique opportunity to delve into fundamental questions in TENGs by manipulating the physical and chemical properties of cellulose materials. This concise critical review aims to thoroughly examine the applications of cellulose materials while shedding light on the opportunities presented by these versatile materials.

Keywords: triboelectric nanogenerators; cellulose; composites

1. The Properties of Cellulose Materials

Cellulose, as a natural product, ubiquitously exists in plants, bacteria, fungi, and other organisms, serving as a fundamental component. Chemically categorized as a polysaccharide chain polymer, the length of the cellulose chain, or molecular weight, is highly dependent on its source of origin (natural length) or the processing method applied (product length). The hydroxyl groups on the glucose in the cellulose chain have the propensity to form hydrogen bonds with the same or adjacent chains, resulting in the formation of nanofibril and microfibril cellulose structures characterized by remarkable mechanical strength. This ability arises from the formation of hydrogen bonds, enabling cellulose fibers to effortlessly create thin films with adjustable tensile strength.

Cellulose manifests in four distinct types [1,2]: cellulose I (I_{α} and I_{β}), II, III, and IV. Type I represents natural cellulose produced by bacteria, algae, and plants. Type II denotes regenerated cellulose obtained through various methods. Types III and IV encompass cellulose subjected to diverse chemical treatments. Figure 1 elucidates the structural variations among these four cellulose types [3]. Table 1 shows the general parameters of different types of nanocellulose materials [4].

The transition of cellulose from type I to type II through regeneration brings about significant alterations in its physical and mechanical properties. These regeneration processes typically involve modifications to cellulose, impacting its solubility. Furthermore, as the regeneration process disassembles cellulose fibers into molecules, it facilitates the production of plastic-like thin films such as cellophane. Most regeneration methods employ reagents to interact with the hydroxyl ($-OH$) groups of cellulose, resulting in the formation of cellulose esters or cellulose ethers. Importantly, these regenerated cellulose materials are predominantly renewable, imparting substantial significance for the future, especially in scenarios where the utilization of engineering polymers is constrained.



Citation: Zhang, R. The Opportunities of Cellulose for Triboelectric Nanogenerators: A Critical Review. *Nanoenergy Adv.* **2024**, *4*, 209–220. <https://doi.org/10.3390/nanoenergyadv4030013>

Academic Editor: Sang Min Lee

Received: 1 December 2023

Revised: 17 January 2024

Accepted: 22 March 2024

Published: 4 July 2024



Copyright: © 2024 by the author. Licensee MDPI, Basel, Switzerland. This article is an open access article distributed under the terms and conditions of the Creative Commons Attribution (CC BY) license (<https://creativecommons.org/licenses/by/4.0/>).

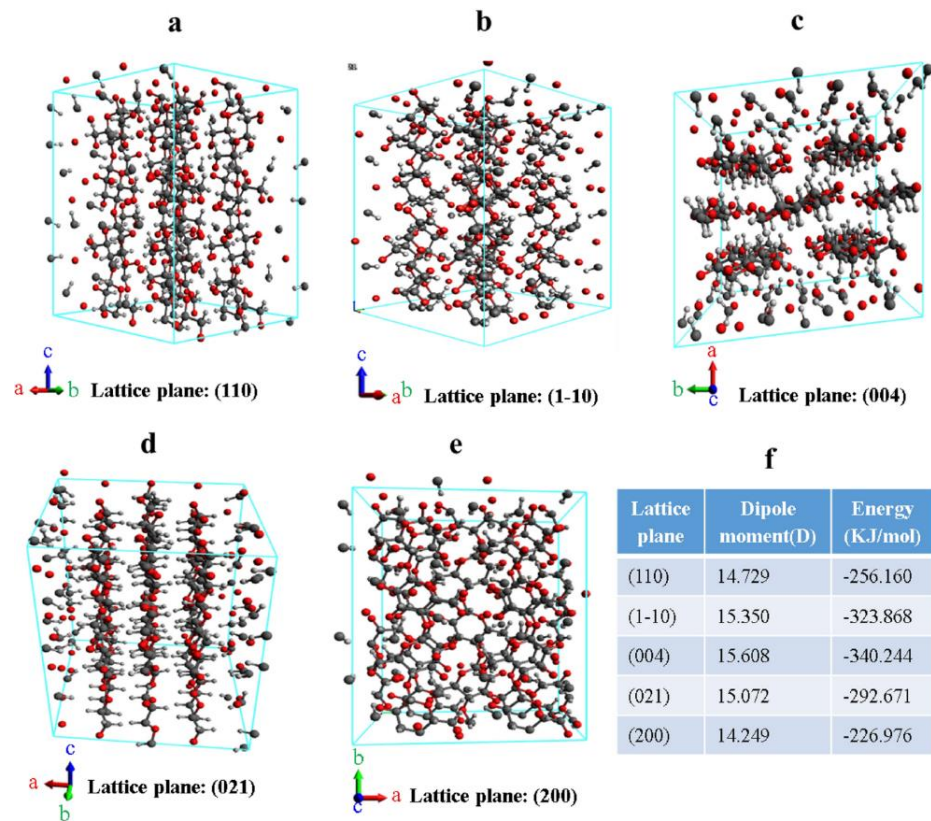


Figure 1. Different types of crystalline cellulose lattice planes and their estimated properties; the figure shows a 2 × 2 × 2 super cell of the cellulose crystal structure with lattice planes (a) 110, (b) 1-10, (c) 004, (d) 021, and (e) 200; a total of 576 atoms and 493 bonds are present in each crystal structure. (f) A table that lists the difference of the dipole moments and energy. Reproduced from ref. [3] under CC by 4.0.

Table 1. Properties and characteristics of nanocellulose substrates reliant on the cellulosic source and defibrillation method. Reused from [4] under CC BY 4.0.

Cellulosic Substrate	Nanocellulose	Preparation Method	Diameter (nm) and Structural Morphology	Average Young's Modulus (GPa)	Apparent Crystallinity (%)	Maximum Degradation Temperature (°C)	Average Tensile Strength (MPa)	Zeta Potential (mV)	References
Comcob residue	CNC	H ₂ SO ₄ hydrolysis	5.5 ± 1.9, short rod-shaped	-	55.9	313	-	-33.8 ± 1.7	Liu et al., 2016
	CNC	Fomic acid hydrolysis	6.5 ± 2.0, long rod-shaped	-	63.8	360	-	-14.3 ± 0.4	
	CNF	TEMPO-mediated oxidation	2.1 ± 1.1, twisted structure	-	49.9	305	-	-23.1 ± 2.3	
	CNF	PFI refining	43.1 ± 25.3, twisted	-	52.1	336	-	-40.3 ± 1.5	
Staliks of wheat straw (<i>Triticum paleas</i>)	CNF	H ₂ SO ₄ hydrolysis and ultrasound treatment	10–40, a mesh-like multilayer structure	11.45	72.5	ca. 400	42.3	-	Barbash et al., 2017
Comhusk	CNC	H ₂ SO ₄ hydrolysis	26.9 ± 3.35, short rod-shaped	-	83.5	351	-	-34.6 ± 2.3	Yang et al., 2017
	CNF	TEMPO-mediated oxidation	10.48 ± 1.83, slender inter-connected webs	-	72.3	279	-	-69.4 ± 1.7	

Table 1. Cont.

Cellulosic Substrate	Nanocellulose	Preparation Method	Diameter (nm) and Structural Morphology	Average Young's Modulus (GPa)	Apparent Crystallinity (%)	Maximum Degradation Temperature (°C)	Average Tensile Strength (MPa)	Zeta Potential (mV)	References
	CNF	High-intensity ultrasonication	20.14 ± 4.32, slender interconnected webs	-	53.4	348	-	-24.3 ± 2.5	
Banane pseudostem	CNF	High-pressure homogenization	30–50, entangled network of polydisperse bundles	-	67.0	337	-	-	Velásquez-Cock et al., 2016
Cotton	CNC	H ₂ PO ₄ hydrolysis	31 ± 14, rod-like shape	-	81.0	325	-	-	Camarero Espinosa et al., 2013
Ushar (<i>Calotropis procera</i>) seed fiber	CNC	H ₂ SO ₄ hydrolysis	14–24, needle shape	-	70.0	ca. 330	-	-	Oun and Rhim, 2016
	CNF	TEMPO-oxidation	10–20, web-like shape	-	59.0	316	-	-	
Bacterial strain <i>Komagataeibacter xylinus</i> (BCC529)	BNC	Static culture for 96 h at 30 °C	29.13 ± 6.53, denser network structure	0.72	47.4	335	0.235	-44.1 ± 0.9	Gao et al., 2020
	BNC	Agitated culture: 300 rpm at 30 °C	29.51 ± 8.03, loose and porous network	-	22.1	310	-	-46.5 ± 1.5	
Kenaf (<i>Hibiscus cannabinus</i> L.) fiber	CNC	H ₂ SO ₄ hydrolysis and ultrasonic treatment	10–28, morphology not defined	-	80.0	ca. 420	61.4	-	Barbash and Yashchenko, 2020

2. The Triboelectric Effect of Cellulose Materials

The triboelectric effect exhibited by cellulose materials has captured researchers' attention since the inception of the first triboelectric series [5]. Early series constructed before 1920 featured cellulose materials represented by wood, paper, and cotton (Table 2). More recently, pure cellulose has been included in triboelectric series [6], revealing a distinct position from the aforementioned cellulose materials. Pure cellulose tends to exhibit a more positive charge in the triboelectric series, potentially influenced by factors such as density and moisture [7,8]. The triboelectric properties of regenerated cellulose vary, depending on the reagents used in the regeneration process, resulting in both more and less positive outcomes compared to pure cellulose.

Recent studies have demonstrated that cellulose can exhibit a higher positive charge affinity than nylon. This heightened positive charge affinity finds explanation through molecular orbital theory. Earlier models, based on molecular orbital theory, described electron transport during triboelectrification, emphasizing the significance of the energy levels of the Highest Occupied Molecular Orbital (HOMO) and Lowest Unoccupied Molecular Orbital (LUMO) in determining the direction of electron transfer. Density Functional Theory (DFT) calculations have revealed proximity in the HOMO and LUMO levels of cellulose and nylon. Consequently, cellulose is anticipated to possess a positive charge affinity akin to nylon. A quantitative assessment of cellulose's triboelectric effect based on triboelectric charge density in 2020 confirmed that regenerated cellulose can indeed exhibit a higher positive charge affinity than nylon [9].

Table 2. Triboelectric series built before 1920 by J. Wilcke, M. Faraday, and P. Shaw [5].

J. Wilcke (1579)	M. Faraday (1840)	P. Shaw (1917)
+	+	+
Glass	Cat's Fur	Glass
Wool	Wool	Wool
Quills	Quills	Cat's fur
Wood	Flint glass	Pb
Paper	Cotton	Silk
Ground glass	Linen	Paper
Pb	Silk	Cotton
Sulfur	Hand	Wood, Fe
Metals	Wood	Ground glass
-	Fe, Cu, Ag, Pb	Resin
	Sulfur	Cu, Ag
	-	Sulfur
		-

3. The Application of Cellulose Materials in TENGs

Numerous studies over the past several years have explored the utilization of cellulose materials as triboelectric layers, with several review articles summarizing these investigations published in the last three years [10–14]. Unlike comprehensive reviews covering all publications, this critical review aims to provide a condensed overview of research conducted with cellulose. Performance evaluations of triboelectric nanogenerators (TENGs) based on cellulose materials are not the focal point of this review. Instead, we delve into the opportunities presented by cellulose for TENGs, outlining key findings and insights in the subsequent section.

4. Paper TENGs

Paper, as one of the most commonly used cellulose materials, has gained interest from researchers for use as triboelectric materials [15] shortly after the invention of TENGs [16]. In this section, paper refers to the commercial paper product but not that made from nanosized cellulose or regenerated cellulose.

Studies on paper-based TENGs have focused on the following:

- Types of electrodes on paper triboelectric material;
- Application of paper-based TENGs;
- Types of paper product used in TENGs.

4.1. Types of Electrodes on Paper Triboelectric Material

Differing from the conventional use of engineering polymers, paper possesses a notably rough surface, facilitating the application of various electrode coatings, such as graphite from diverse sources. Graphite paper can be directly affixed to the rear surface of a paper tribo-layer, functioning akin to metal-film-based electrodes. An innovative approach involves using a pencil to “draw” a graphite electrode layer on paper [17]. Alternatively, one can create an electron-conductive layer on paper using a rollerball pen filled with a conductive ink comprising silver nanowires and graphene oxide [17]. Furthermore, inkjet printing techniques with carbon nanotube/silver nanowire ink enable the printing of conductive layers on paper [18]. These electrode variations offer the coated tribo-layer enhanced flexibility and foldability compared to conventional metal tapes. This attribute expands the potential applications of paper-based triboelectric nanogenerators (TENGs) across numerous scenarios [19–24].

4.2. Application of Paper-Based TENGs

- Energy Harvesting:

Paper-based triboelectric nanogenerators (TENGs) find applications in energy harvesting, self-powered sensing, and more. Printer paper and copy paper are predominant choices for these devices. A comprehensive list detailing the performance metrics of paper-based TENGs is available in a review by Liang et al. [25]. Typically, the highest power densities achieved by paper-based TENGs range in the tens of W/m^2 [26,27], with no instances surpassing $100 W/m^2$. In comparison to TENGs based on engineering polymers, the performance of paper-based counterparts is constrained by the paper's relatively weak charge affinity.

Exploiting the flexibility, foldability, and tailorability of paper, researchers can construct origami-inspired TENGs. These origami structures often integrate multiple TENGs to enhance the volume power density. Commonly employed origami shapes in paper-based TENGs include zigzag, slinky, and rhombic configurations [28–31].

- Self-Powered Sensing:

In addition to energy harvesting, the development of self-powered sensing systems has garnered increasing attention from researchers. Paper-based triboelectric nanogenerator (TENG) sensors are particularly noteworthy due to paper's environmentally friendly and biodegradable nature, as well as its flexibility and foldability. In comparison to engineering polymers, paper is abundantly produced, rendering paper-based TENG sensors a more cost-effective option. Although the application scenarios for paper-based TENG sensors are similar to those using engineering-polymer-based TENGs, a unique example involves the utilization of paper-based TENGs for sound sensing [15]. This application provides a cost-effective approach to audio sensing.

- Extend the Lifecycle of Paper Products:

Introducing a novel stage in the product lifecycle could substantially enhance its value, contributing significantly to sustainable development. A recent study by Zhang et al. [27] highlights the utilization of wastepaper as a basis for a high-performance triboelectric nanogenerator (TENG) designed for energy harvesting. This innovative TENG boasts a remarkable maximum power density exceeding $43 W/m^2$, making it suitable for powering small electronics. Expanding this concept to various types of wastepaper products holds promise, not only as triboelectric layers but also as supportive substrates within TENGs. This approach aligns with the principles of sustainable development by repurposing waste materials, offering an environmentally friendly and resource-efficient solution in the realm of energy harvesting technology.

5. Nanocellulose-Based TENGs

In addition to conventional commercial paper products, nanocellulose variants like nanofibrillated cellulose (NFC), bacterial cellulose (BC), and cellulose nanofibrils (CNFs) have garnered increased attention. These nanocellulose-based triboelectric layers offer a laboratory-friendly platform with controllable properties, including nanocellulose size and film thickness. A comprehensive 2021 review [32] provides systematic insights into nanocellulose applications in triboelectric nanogenerators (TENGs), offering detailed information.

Notably, nanocellulose facilitates the fabrication of both 2D [33] and 3D [34] structures, expanding the potential application scenarios. An innovative aspect involves modifying nanocellulose to tailor the triboelectric effect. While pristine cellulose exhibits a high positive charge affinity, surface modifications, such as introducing fluorine groups [35], enable the creation of nanocellulose with a higher negative charge affinity. This advancement allows the production of all-cellulose-based TENGs with impressive performance [36].

The exploration of nanocellulose composites presents another avenue of interest in TENGs. Nanocellulose's chemical activity, stemming from hydroxyl groups on the chain, enables effective composite formation with both organic and inorganic materials. Methods

such as mixing a nanocellulose suspension with other materials [37], dispersing materials in a nanocellulose solution [38], and layer-by-layer film [39] production have been explored for nanocomposite fabrication. While these methods lack precise control over nanocellulose-component interactions, they demonstrate particular efficacy in compositing nanocellulose with inorganic materials [38].

When it comes to compositing with organic materials, the interaction between nanocellulose and other components becomes a crucial consideration. Utilizing hydrogen bonds between nanocellulose and other materials, which require no chemical reactions or reagents, stands out as the simplest method for producing nanocellulose–organic composites [40]. Another approach involves polymerization, creating covalent bonds through chemical reactions [41,42]. The third method employs a link molecule to interact with both nanocellulose and the other component polymer; for instance, aminoguanidine hydrochloride (AGH) has been used to link nanocellulose and polyethylene oxide (PEO) [43].

Nanocellulose composites hold significant potential in triboelectric nanogenerators (TENGs) for several reasons:

- Altering surface properties, such as hydrophobicity [44];
- Enhancing charge generation;
- Modifying permittivity.

Naturally hydrophilic cellulose tends to attract moisture from the air, diminishing charge accumulation on the surface during triboelectrification. Compositing with other materials, like ferroelectric BaTiO₃ materials, has been shown to significantly enhance charge generation in the composite film [45]. The aligned dipoles in the BaTiO₃ domains induce a net electric field, thereby improving charge transfer.

Moreover, changing permittivity through composite materials can substantially enhance the performance of nanocellulose-based TENGs. Theoretical simulations, discussed by Zhang, emphasize the importance of permittivity changes based on the current density equation of triboelectric nanogenerators under a contact-separation mode [46]. Alterations in permittivity by composites affect the electrostatic induction part of the equation, consequently influencing the TENGs' output (Figure 2). In many cases, inorganic materials like BaTiO₃ [45], MXene [37], and carbon nanotubes [42] are employed to tune dielectric properties.

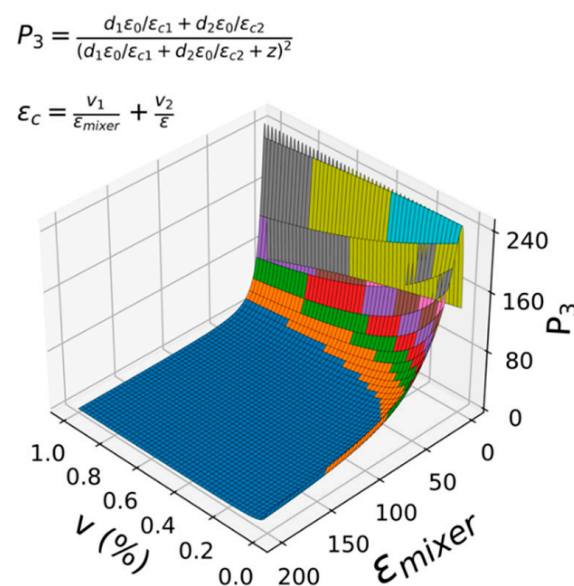


Figure 2. Cont.

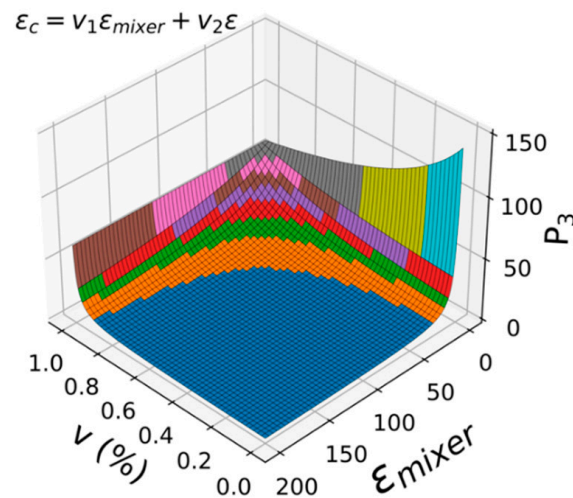


Figure 2. Simulated P3 values based on the series mixing model (**top**) and the simplified model (**bottom**). v_1 and v_2 are the volume fractions of the components in a nanocomposite, and $v_1 + v_2 = 1$. The thicknesses of the dielectric materials, d_1 and d_2 , were set at 0.1 mm, and the distance, z , between the triboelectric surfaces was set at 1 mm. Reproduced from ref. [46] under CC by 4.0.

6. Regenerated Cellulose-Based TENGs

In contrast to the fiber-shaped nanocellulose, regenerated cellulose is a molecule produced by breaking down cellulose fibers using chemicals. Consequently, films made of nanocellulose and regenerated cellulose exhibit notable distinctions. Nanocellulose films appear dense with percolations, while regenerated cellulose films resemble those of engineering polymers.

Studies on regenerated cellulose reveal variations arising from modifications to the polysaccharide chain. Examples include cellophane and cellulose acetate, each with distinct mechanical, chemical, and electrostatic properties due to specific chemical group modifications on the chain. For instance, cellophane exhibits a neutral triboelectric charge density [9], whereas cellulose acetate displays a highly negative charge density [47].

Recent findings challenge the conventional belief of regenerated cellulose exhibiting low positive charge affinity, as it demonstrates unexpectedly high positive charge affinity. This elevated affinity is attributed to the relatively high Highest Occupied Molecular Orbital (HOMO) and Lowest Unoccupied Molecular Orbital (LUMO) orbitals that closely resemble nylon. The high positive charge affinity allows regenerated cellulose films to function as excellent triboelectric layers. A recent report introduces a fully green TENG by coupling a regenerated cellulose film with another, more negative regenerated cellulose film, such as cellophane [9].

Similar to nanocellulose, regenerated cellulose is often combined with other materials using physical and chemical crosslinking strategies [48]. Physical strategies involve hydrogen bonding, ionic interactions, host–guest interactions, and hydrophobic interactions, while chemical strategies include reversible and irreversible chemical crosslinking, such as the Schiff base reaction, disulfide bond formation, esterification, and epoxide. Irradiation crosslinking and semi/full-interpenetrating polymer networks are also effective methods for modifying cellulose. A figure depicting commonly used crosslinking strategies can be found in Figure 3 [48]. Additionally, the direct mixing of materials with regenerated cellulose dispersion has been reported to produce composites [49], a method more suitable for generating regenerated cellulose–inorganic nanomaterial composites [49–51].

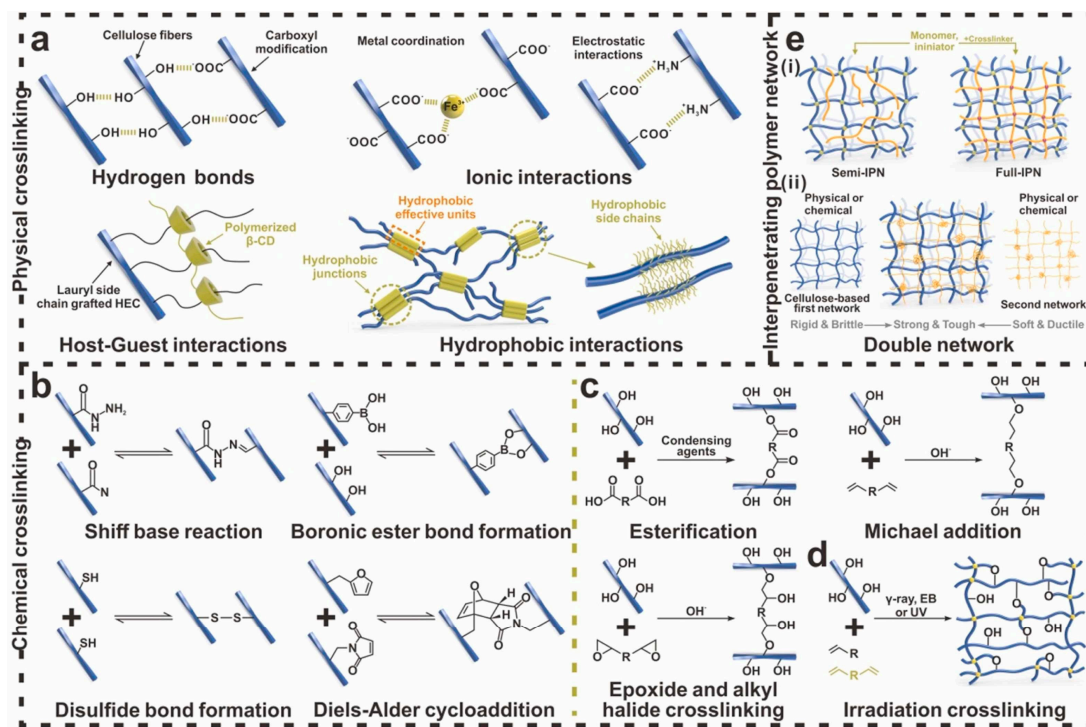


Figure 3. Crosslinking strategies of cellulosic hydrogels. (a) Physical crosslinking, including hydrogen bonding, ionic interactions, host–guest interactions, hydrophobic interactions, etc. (b) Reversible chemical crosslinking, including Schiff base reaction, boronic ester bond formation, disulfide bond formation, Diels–Alder cycloaddition, etc. (c) Irreversible chemical crosslinking, including esterification, Michael addition, epoxide and alkyl halide crosslinking, etc. (d) Irradiation crosslinking, including γ -ray, electron beam (EB), and ultraviolet (UV). (e) Semi/full-interpenetrating polymer network (IPN) and double network (DN). Reproduced with permission from Ref. [48]. Copyright 2023, Elsevier.

The performances of regenerated cellulose-based TENGs generally align with those of nanocellulose-based TENGs. For detailed performance metrics, readers are referred to several comprehensive review papers [32,48,52], as they are not included in this critical review.

7. The Opportunities of Cellulose Materials for TENGs

Numerous studies have delved into the fundamentals of triboelectrification, focusing on charge transport and density. However, the molecular structures of triboelectric materials, crucial determinants of the triboelectric process, have often been overlooked. This neglect arises from the limited flexibility in the crystalline structure and the chemical activities of engineering polymers. To bridge this gap, we propose several avenues for systematic exploration:

- **Functional Group Influence on Triboelectric Effect:**

Exploiting the hydroxyl groups on the cellulose chain offers opportunities for functionalization with various reagents, providing insights into how chain length and terminal groups influence the triboelectric effect (Figure 4). Modifying the cellulose chain with molecules of different lengths (e.g., polyethylene) allows a nuanced understanding of how chain length impacts the triboelectric effect. Altering terminal groups on the modified cellulose chain elucidates the triboelectric effects of functional groups, contributing to an in-depth comprehension of differences among engineering polymers.

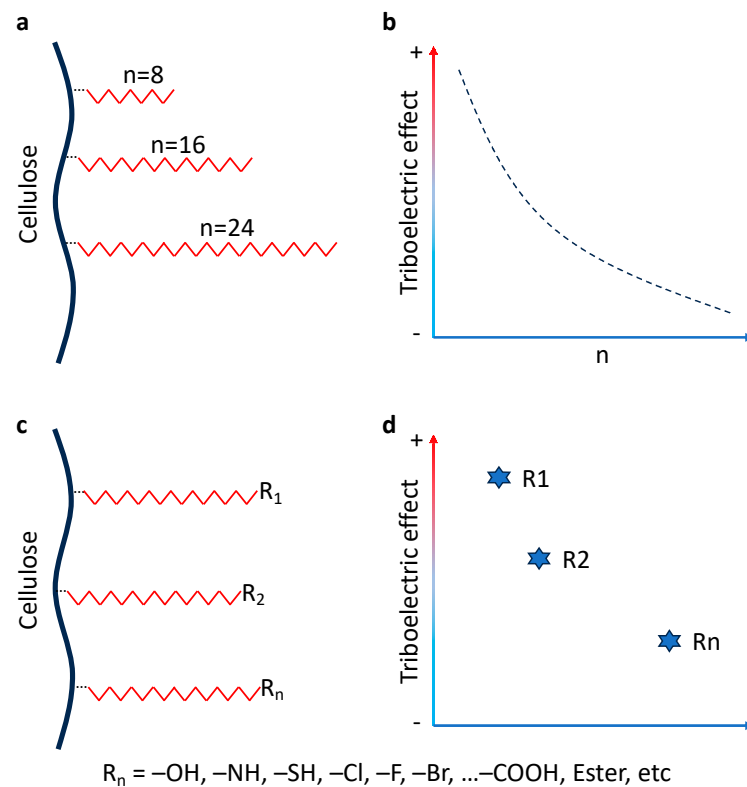


Figure 4. Functionalization of cellulose towards stronger triboelectric effect. (a) Modification to the side chain of cellulose with the same type of molecule but with different lengths of carbon chain. (b) An expected change in triboelectric effect changes with different lengths of the carbon chain. (c) Modification to the side chain of cellulose with molecules with only differences at one terminal. (d) An expected change in triboelectric effect changes with different terminal groups.

- **Crystal Structure Influence on Triboelectric Effect:**

Cellulose exhibits four distinct crystalline structures, each possessing different surface groups with varying charge affinity. Systematic studies on the triboelectric effects of these structures can unravel correlations between charge affinity and surface groups/atoms.

- **Impact of Fiber Size on Triboelectric Effect:**

Unlike engineering polymers, cellulose can be shaped in various forms, allowing for systematic studies on how fiber sizes (ranging from 10 nm to micrometers) influence triboelectric effects. Cellulose's unique property enables researchers to explore the impact of sizes, especially in yarns ranging from micrometers to millimeters.

- **Innovative Applications:**

Leveraging cellulose's chemical activity, cellulose-based TENGs can serve as excellent triboelectric materials for chemical sensing applications, capitalizing on hydrogen bonding between cellulose's hydroxyl groups and target molecules. The 3D structure of cellulose opens possibilities for TENGs not only as sensors but also as absorbers for targeted molecules.

- **Towards Green Triboelectric Nanogenerators:**

As a natural material, cellulose emerges as a crucial component in fabricating green triboelectric nanogenerators (TENGs), addressing environmental concerns associated with plastic materials.

The negligible environmental impact and biodegradability of cellulose, especially regenerated and modified cellulose, make it a promising candidate for fabricating high-performance, environmentally friendly TENGs.

8. Conclusions

This review provides an overview of recent studies on cellulose-based TENGs, highlighting discoveries such as cellulose's high positive charge affinity, crystal structures, and applications in energy harvesting, self-powered sensors, and the contribution to sustainable development by extending the lifecycle of paper products. We have also outlined opportunities for future research of cellulose-based TENGs and suggested different strategies for both fundamental and experimental studies. This critical review not only provides an overview of the application of cellulose in TENGs, but also emphasizes the multifaceted potential of cellulose in advancing TENG technology.

Funding: This work was financially supported by the Swedish Research Council, Stiftelsen Promobilia, and the Knowledge Foundation of Sweden.

Data Availability Statement: No new data were created or analyzed in this study. Data sharing is not applicable to this article.

Conflicts of Interest: The author declares no conflict of interest.

References

1. Fu, L.-H.; Liu, B.; Meng, L.-Y.; Ma, M.-G. Comparative Study of Cellulose/Ag Nanocomposites Using Four Cellulose Types. *Mater. Lett.* **2016**, *171*, 277–280. [\[CrossRef\]](#)
2. Zugenmaier, P. Conformation and Packing of Various Crystalline Cellulose Fibers. *Prog. Polym. Sci.* **2001**, *26*, 1341–1417. [\[CrossRef\]](#)
3. Thulluri, C.; Balasubramaniam, R.; Velankar, H. Generation of highly amenable cellulose-I β via selective delignification of rice straw using a reusable cyclic ether-assisted deep eutectic solvent system. *Sci. Rep.* **2021**, *11*, 1591. [\[CrossRef\]](#)
4. Trache, D.; Tarchoun, A.F.; Derradji, M.; Hamidon, T.S.; Masruchin, N.; Brosse, N.; Hussin, M.H. Nanocellulose: From Fundamentals to Advanced Applications. *Front. Chem.* **2020**, *8*, 392. [\[CrossRef\]](#)
5. Shaw, P.E. Experiments on Tribo-Electricity. I.—The Tribo-Electric Series. *Proc. R. Soc. Lond. Ser. A Contain. Pap. A Math. Phys. Character* **1917**, *94*, 16–33. [\[CrossRef\]](#)
6. Choi, Y.S.; Kar-Narayan, S. Nylon-11 Nanowires for Triboelectric Energy Harvesting. *EcoMat* **2020**, *2*, e12063. [\[CrossRef\]](#)
7. Zhang, R.; Olin, H. Material Choices for Triboelectric Nanogenerators: A Critical Review. *EcoMat* **2020**, *2*, e12062. [\[CrossRef\]](#)
8. Liu, Y.; Mo, J.; Fu, Q.; Lu, Y.; Zhang, N.; Wang, S.; Nie, S. Enhancement of Triboelectric Charge Density by Chemical Functionalization. *Adv. Funct. Mater.* **2020**, *30*, 2004714. [\[CrossRef\]](#)
9. Zhang, R.; Dahlström, C.; Zou, H.; Jonzon, J.; Hummelgård, M.; Örtengren, J.; Blomquist, N.; Yang, Y.; Andersson, H.; Olsen, M.; et al. Cellulose-Based Fully Green Triboelectric Nanogenerators with Output Power Density of 300 W m⁻². *Adv. Mater.* **2020**, *32*, 2002824. [\[CrossRef\]](#)
10. Tang, Q.; Guo, H.; Yan, P.; Hu, C. Recent Progresses on Paper-based Triboelectric Nanogenerator for Portable self-powered Sensing Systems. *EcoMat* **2020**, *2*, e12060. [\[CrossRef\]](#)
11. Wang, X.; Yao, C.; Wang, F.; Li, Z. Cellulose-Based Nanomaterials for Energy Applications. *Small* **2017**, *13*, 1702240. [\[CrossRef\]](#)
12. Zhang, M.; Du, H.; Liu, K.; Nie, S.; Xu, T.; Zhang, X.; Si, C. Fabrication and Applications of Cellulose-Based Nanogenerators. *Adv. Compos. Hybrid Mater.* **2021**, *4*, 865–884. [\[CrossRef\]](#)
13. Niu, Z.; Cheng, W.; Cao, M.; Wang, D.; Wang, Q.; Han, J.; Long, Y.; Han, G. Recent Advances in Cellulose-Based Flexible Triboelectric Nanogenerators. *Nano Energy* **2021**, *87*, 106175. [\[CrossRef\]](#)
14. Zhou, J.; Wang, H.; Du, C.; Zhang, D.; Lin, H.; Chen, Y.; Xiong, J. Cellulose for Sustainable Triboelectric Nanogenerators. *Adv. Energy Sustain. Res.* **2022**, *3*, 2100161. [\[CrossRef\]](#)
15. Fan, X.; Chen, J.; Yang, J.; Bai, P.; Li, Z.; Wang, Z.L. Ultrathin, Rollable, Paper-Based Triboelectric Nanogenerator for Acoustic Energy Harvesting and Self-Powered Sound Recording. *ACS Nano* **2015**, *9*, 4236–4243. [\[CrossRef\]](#)
16. Fan, F.-R.; Tian, Z.-Q.; Wang, Z.L. Flexible Triboelectric Generator. *Nano Energy* **2012**, *1*, 328–334. [\[CrossRef\]](#)
17. Zhang, X.-S.; Su, M.; Brugger, J.; Kim, B. Penciling a Triboelectric Nanogenerator on Paper for Autonomous Power MEMS Applications. *Nano Energy* **2017**, *33*, 393–401. [\[CrossRef\]](#)
18. Choi, K.-H.; Yoo, J.; Lee, C.K.; Lee, S.-Y. All-Inkjet-Printed, Solid-State Flexible Supercapacitors on Paper. *Energy Environ. Sci.* **2016**, *9*, 2812–2821. [\[CrossRef\]](#)
19. Wu, C.; Kima, T.W.; Sung, S.; Park, J.H.; Li, F. Ultrasoft and Cuttable Paper-Based Triboelectric Nanogenerators for Mechanical Energy Harvesting. *Nano Energy* **2018**, *44*, 279–287. [\[CrossRef\]](#)
20. Ankanahalli Shankaregowda, S.; Sagade Muktar Ahmed, R.F.; Nanjegowda, C.B.; Wang, J.; Guan, S.; Puttaswamy, M.; Amini, A.; Zhang, Y.; Kong, D.; Sannathammegowda, K.; et al. Single-Electrode Triboelectric Nanogenerator Based on Economical Graphite Coated Paper for Harvesting Waste Environmental Energy. *Nano Energy* **2019**, *66*, 104141. [\[CrossRef\]](#)
21. Xia, K.; Du, C.; Zhu, Z.; Wang, R.; Zhang, H.; Xu, Z. Sliding-Mode Triboelectric Nanogenerator Based on Paper and as a Self-Powered Velocity and Force Sensor. *Appl. Mater. Today* **2018**, *13*, 190–197. [\[CrossRef\]](#)

22. Wu, C.; Park, J.H.; Sung, S.; Koo, B.; Lee, Y.H.; Kim, T.W. Integrable Card-Type Triboelectric Nanogenerators Assembled by Using Less Problematic, Readily Available Materials. *Nano Energy* **2018**, *51*, 383–390. [[CrossRef](#)]
23. Song, J.; Gao, L.; Tao, X.; Li, L. Ultra-Flexible and Large-Area Textile-Based Triboelectric Nanogenerators with a Sandpaper-Induced Surface Microstructure. *Materials* **2018**, *11*, 2120. [[CrossRef](#)]
24. Wu, C.; Wang, X.; Lin, L.; Guo, H.; Wang, Z.L. Paper-Based Triboelectric Nanogenerators Made of Stretchable Interlocking Kirigami Patterns. *ACS Nano* **2016**, *10*, 4652–4659. [[CrossRef](#)]
25. Liang, S.; Wang, Y.; Liu, Q.; Yuan, T.; Yao, C. The Recent Progress in Cellulose Paper-Based Triboelectric Nanogenerators. *Adv. Sustain. Syst.* **2021**, *5*, 2100034. [[CrossRef](#)]
26. Mao, Y.; Zhang, N.; Tang, Y.; Wang, M.; Chao, M.; Liang, E. A Paper Triboelectric Nanogenerator for Self-Powered Electronic Systems. *Nanoscale* **2017**, *9*, 14499–14505. [[CrossRef](#)]
27. Zhang, R.; Hummelgård, M.; Örtengren, J.; Andersson, H.; Olsen, M.; Chen, W.; Wang, P.; Dahlström, C.; Eivazi, A.; Norgren, M. Energy Harvesting Using Wastepaper-Based Triboelectric Nanogenerators. *Adv. Eng. Mater.* **2023**, *25*, 2300107. [[CrossRef](#)]
28. Yang, H.; Deng, M.; Tang, Q.; He, W.; Hu, C.; Xi, Y.; Liu, R.; Wang, Z.L. A Nonencapsulative Pendulum-Like Paper-Based Hybrid Nanogenerator for Energy Harvesting. *Adv. Energy Mater.* **2019**, *9*, 1901149. [[CrossRef](#)]
29. Li, S. Double-Folding Paper-Based Generator for Mechanical Energy Harvesting. *Front. Optoelectron.* **2017**, *10*, 38–43. [[CrossRef](#)]
30. Yang, P.-K.; Lin, Z.-H.; Pradel, K.C.; Lin, L.; Li, X.; Wen, X.; He, J.-H.; Wang, Z.L. Paper-Based Origami Triboelectric Nanogenerators and Self-Powered Pressure Sensors. *ACS Nano* **2015**, *9*, 901–907. [[CrossRef](#)] [[PubMed](#)]
31. Zhang, H.; Wang, H.; Zhang, J.; Zhang, Z.; Yu, Y.; Luo, J.; Dong, S. A Novel Rhombic-Shaped Paper-Based Triboelectric Nanogenerator for Harvesting Energy from Environmental Vibration. *Sens. Actuators A Phys.* **2020**, *302*, 111806. [[CrossRef](#)]
32. Vatankhah, E.; Tadayon, M.; Ramakrishna, S. Boosted Output Performance of Nanocellulose-Based Triboelectric Nanogenerators via Device Engineering and Surface Functionalization. *Carbohydr. Polym.* **2021**, *266*, 118120. [[CrossRef](#)] [[PubMed](#)]
33. Wang, Q.; Yao, Q.; Liu, J.; Sun, J.; Zhu, Q.; Chen, H. Processing Nanocellulose to Bulk Materials: A Review. *Cellulose* **2019**, *26*, 7585–7617. [[CrossRef](#)]
34. Dufresne, A. Nanocellulose: A New Ageless Bionanomaterial. *Mater. Today* **2013**, *16*, 220–227. [[CrossRef](#)]
35. Nie, S.; Fu, Q.; Lin, X.; Zhang, C.; Lu, Y.; Wang, S. Enhanced Performance of a Cellulose Nanofibrils-Based Triboelectric Nanogenerator by Tuning the Surface Polarizability and Hydrophobicity. *Chem. Eng. J.* **2021**, *404*, 126512. [[CrossRef](#)]
36. Yao, C.; Yin, X.; Yu, Y.; Cai, Z.; Wang, X. Chemically Functionalized Natural Cellulose Materials for Effective Triboelectric Nanogenerator Development. *Adv. Funct. Mater.* **2017**, *27*, 1700794. [[CrossRef](#)]
37. Yang, W.; Chen, H.; Wu, M.; Sun, Z.; Gao, M.; Li, W.; Li, C.; Yu, H.; Zhang, C.; Xu, Y.; et al. A Flexible Triboelectric Nanogenerator Based on Cellulose-Reinforced MXene Composite Film. *Adv. Mater. Interfaces* **2022**, *9*, 2102124. [[CrossRef](#)]
38. Zhan, Y.; Meng, Y.; Li, W.; Chen, Z.; Yan, N.; Li, Y.; Teng, M. Magnetic Recoverable MnFe₂O₄/Cellulose Nanocrystal Composites as an Efficient Catalyst for Decomposition of Methylene Blue. *Ind. Crops Prod.* **2018**, *122*, 422–429. [[CrossRef](#)]
39. Sriphan, S.; Charoonsuk, T.; Maluangnont, T.; Pakawanit, P.; Rojviriyi, C.; Vittayakorn, N. Multifunctional Nanomaterials Modification of Cellulose Paper for Efficient Triboelectric Nanogenerators. *Adv. Mater. Technol.* **2020**, *5*, 2000001. [[CrossRef](#)]
40. Wu, S.; Li, G.; Liu, W.; Yu, D.; Li, G.; Liu, X.; Song, Z.; Wang, H.; Liu, H. Fabrication of Polyethyleneimine-Paper Composites with Improved Tribopositivity for Triboelectric Nanogenerators. *Nano Energy* **2022**, *93*, 106859. [[CrossRef](#)]
41. Wang, X.; Li, X.; Wang, B.; Chen, J.; Zhang, L.; Zhang, K.; He, M.; Xue, Y.; Yang, G. Preparation of Salt-Induced Ultra-Stretchable Nanocellulose Composite Hydrogel for Self-Powered Sensors. *Nanomaterials* **2022**, *13*, 157. [[CrossRef](#)] [[PubMed](#)]
42. Wang, Z.; Chen, C.; Fang, L.; Cao, B.; Tu, X.; Zhang, R.; Dong, K.; Lai, Y.-C.; Wang, P. Biodegradable, Conductive, Moisture-Proof, and Dielectric Enhanced Cellulose-Based Triboelectric Nanogenerator for Self-Powered Human-Machine Interface Sensing. *Nano Energy* **2023**, *107*, 108151. [[CrossRef](#)]
43. Lin, C.; Zhao, H.; Huang, H.; Ma, X.; Cao, S. PEO/Cellulose Composite Paper Based Triboelectric Nanogenerator and Its Application in Human-Health Detection. *Int. J. Biol. Macromol.* **2023**, *228*, 251–260. [[CrossRef](#)] [[PubMed](#)]
44. Li, E.; Pan, Y.; Wang, C.; Liu, C.; Shen, C.; Pan, C.; Liu, X. Multifunctional and Superhydrophobic Cellulose Composite Paper for Electromagnetic Shielding, Hydraulic Triboelectric Nanogenerator and Joule Heating Applications. *Chem. Eng. J.* **2021**, *420*, 129864. [[CrossRef](#)]
45. Oh, H.; Kwak, S.S.; Kim, B.; Han, E.; Lim, G.; Kim, S.; Lim, B. Highly Conductive Ferroelectric Cellulose Composite Papers for Efficient Triboelectric Nanogenerators. *Adv. Funct. Mater.* **2019**, *29*, 1904066. [[CrossRef](#)]
46. Pecunia, V.; Silva, S.R.P.; Phillips, J.D.; Artegiani, E.; Romeo, A.; Shim, H.; Park, J.; Kim, J.H.; Yun, J.S.; Welch, G.C.; et al. Roadmap on Energy Harvesting Materials. *J. Phys. Mater.* **2023**, *6*, 042501. [[CrossRef](#)] [[PubMed](#)]
47. Zou, H.; Zhang, Y.; Guo, L.; Wang, P.; He, X.; Dai, G.; Zheng, H.; Chen, C.; Wang, A.C.; Xu, C.; et al. Quantifying the Triboelectric Series. *Nat. Commun.* **2019**, *10*, 1427. [[CrossRef](#)] [[PubMed](#)]
48. Qin, Y.; Zhang, W.; Liu, Y.; Zhao, J.; Yuan, J.; Chi, M.; Meng, X.; Du, G.; Cai, C.; Wang, S.; et al. Cellulosic Gel-Based Triboelectric Nanogenerators for Energy Harvesting and Emerging Applications. *Nano Energy* **2023**, *106*, 108079. [[CrossRef](#)]
49. Shi, K.; Huang, X.; Sun, B.; Wu, Z.; He, J.; Jiang, P. Cellulose/BaTiO₃ Aerogel Paper Based Flexible Piezoelectric Nanogenerators and the Electric Coupling with Triboelectricity. *Nano Energy* **2019**, *57*, 450–458. [[CrossRef](#)]
50. Sardana, S.; Kaur, H.; Arora, B.; Aswal, D.K.; Mahajan, A. Self-Powered Monitoring of Ammonia Using an MXene/TiO₂/Cellulose Nanofiber Heterojunction-Based Sensor Driven by an Electrospun Triboelectric Nanogenerator. *ACS Sens.* **2022**, *7*, 312–321. [[CrossRef](#)]

51. Chen, S.; Li, J.; Song, Y.; Yang, Q.; Shi, Z.; Xiong, C. Flexible and Environment-Friendly Regenerated Cellulose/MoS₂ Nanosheet Nanogenerators with High Piezoelectricity and Output Performance. *Cellulose* **2021**, *28*, 6513–6522. [[CrossRef](#)]
52. Song, Y.; Shi, Z.; Hu, G.-H.; Xiong, C.; Isogai, A.; Yang, Q. Recent Advances in Cellulose-Based Piezoelectric and Triboelectric Nanogenerators for Energy Harvesting: A Review. *J. Mater. Chem. A* **2021**, *9*, 1910–1937. [[CrossRef](#)]

Disclaimer/Publisher's Note: The statements, opinions and data contained in all publications are solely those of the individual author(s) and contributor(s) and not of MDPI and/or the editor(s). MDPI and/or the editor(s) disclaim responsibility for any injury to people or property resulting from any ideas, methods, instructions or products referred to in the content.